Progress In Electromagnetics Research B, Vol. 10, 117–130, 2008

THE SINGULARITY PROBLEM AT THE WIRE/SURFACE JUNCTION REGION FOR ANTENNA AND ARRAYS WITH BODIES OF REVOLUTION

X. Cao and J. Gao

Telecommunication Engineering Institute
Air Force Engineering University of CPLA
Shaanxi 710077, P. R. China

Abstract—In this paper, a fast and efficient method based on MOM is proposed for the analysis of antenna and array mounted on bodies of revolution. An attachment mode is introduced to ensure the continuity of current density at the junction region between wire antenna and cylindrical surface. A method based on suitable changes of coordinates and domains is presented to extract singular point of the self-impedance element calculation at junction region and accurate impedance can be obtained. Taking the antennas and array mounted on a finite solid conducting cylinder as an example, the impedance characteristics and radiation pattern are calculated. The good agreement between the results obtained by using the analysis method presented in this paper and those of CST and NEC software reveals the accuracy and high efficiency of this method.

1. INTRODUCTION

The body of revolution is a familiar geometry. It is widely used in aircraft, such as missile, rocket, artificial-satellite. As the geometry is designed in streamline, it has good air-dynamics characteristics. Research shows that the curvature radius of the cylinder has an effect on the radiation pattern [1, 2]. As the mobile communication is prospering with each passing day, the antennas and array with the body of revolution have been widely applied to mobile communication systems due to their advantages, for example, when applied to a base station, compared with the plane antenna, the antennas and array with the body of revolution can lead to a easier access to the communication smart antenna. In order to enhance the computational efficiency of antennas and array with the body of revolution, the surface currents

of the cylinder are expanded as overlapping triangular functions and complex Fourier mode. It is an efficient procedure to reduce the order of matrix in MOM and the computing time and storage required [3–6]. But the efficiency and accuracy of computation results are hindered because of the singularity that appears in impedance matrix elements. When it comes to the singularity problem of the impedance matrix elements for the revolution body and wire antenna in MOM, there are a lot of literature report [1–9], but there is little information considering the singularity of the computation of self-impedance at the junction region between wire antenna and cylinder surface. In this paper, a rigorous method is firstly introduced to extract the singularity of the Greens function appearing within the integrands of the self-impedance element at the junction region between wire antenna and cylindrical surface, and the effect of the size of the junction region on the cylinder surface on the self-impedance of the attachment point is analysed. The input impedance and radiation pattern of wire antenna and patch array of an L-probe feed mounted on the finite solid cylinder obtained by the method in this paper agree well with the CST and NEC results.

2. THEORY

The geometry model of wire antenna with revolution body as shown in Fig. 1, in terms of the enforcing the boundary condition $\vec{E}^{i}(\vec{r})\Big|_{\tan} +$

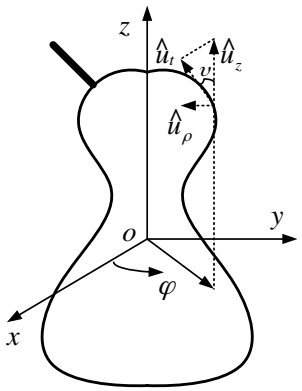

Figure 1. The geometry model of revolution body.

$\vec{E}^{s}\left(\vec{r}\right)\Big|_{\tan}=0$, so

$$\vec{E}^{i}\left(\vec{r}\right)\Big|_{\tan} = -\vec{E}^{s}\left(\vec{r}\right)\Big|_{\tan} = j\omega\mu\iint\limits_{S}\vec{J}\left(\vec{r}'\right)G\left(\vec{R}\right)ds' - \frac{1}{j\omega\varepsilon}\nabla'_{s}\iint\limits_{S}\left[\nabla\cdot\vec{J}\left(\vec{r}'\right)\right]G\left(\vec{R}\right)ds' \quad (1)$$

In which $\vec{R}=\vec{r}-\vec{r}'$ is the vector distance between the source point $\vec{r}'$ to the observation point $\vec{r}$, $R=\left|\vec{R}\right|=\sqrt{r'^2+r^2-2r'r\cos(\varphi-\varphi')}$, and $G\left(R\right)=e^{-jkR}/4\pi R$ is the free-space Green's function. $\vec{J}\left(\vec{r}'\right)$ is the surface current density on the conducting.

$$\vec{J}\left(\vec{r}'\right)=\vec{J}^{s}\left(\vec{r}'\right)+\vec{J}^{w}\left(\vec{r}'\right)+\vec{J}^{A}\left(\vec{r}'\right) \quad (2)$$

In which $\vec{J}^{s}\left(\vec{r}'\right)$, $\vec{J}^{w}\left(\vec{r}'\right)$, and $\vec{J}^{A}\left(\vec{r}'\right)$ represent the current density on the cylinder surface, wire antenna and junction region between wire and cylinder surface, respectively.

Considering the rotational symmetry geometry characteristic of the revolution body, the equivalent current is a vector quantity and can be expressed as a superposition of two orthogonal vectors at any points on the surface. The obvious choice for the current vectors is surface tangential vector $\hat{u}_t$, which is rotationally symmetric about the angle φ, and the azimuthal vector $\hat{u}_\varphi$. Therefore the surface current density of the revolution body can be expressed as follows

$$\vec{J}=J^{t}\hat{u}_t+J^{\varphi}\hat{u}_\varphi=\sum_{i=1}^{M}\sum_{n=-N}^{N}\left(I_{ni}^{st}\vec{J}_{ni}^{st}+I_{ni}^{s\phi}\vec{J}_{ni}^{s\phi}\right) \quad (\mathrm{A/m^2}) \quad (3)$$

$$\begin{cases}\vec{J}_{ni}^{t}=\hat{u}_{ti}\dfrac{T(t-t_i)}{\rho}e^{jn\phi}\\ \vec{J}_{ni}^{\phi}=\hat{u}_{\varphi i}\dfrac{T(t-t_i)}{\rho}e^{jn\phi}\end{cases} \quad (4)$$

where $\hat{u}_{ti}$ and $\hat{u}_{\varphi i}$ are the unit vectors along t and φ direction, and ρ is the radius of the revolution body, $T(t-t_i)$ is the triangle base function about the ith segment, the subscript n denote the Fourier mode number along φ direction in MOM.

For wire antenna, suppose the currents distribution $\vec{J}_w$ on wire antenna is expanded with piecewise triangular basis functions.

$$\vec{J}^{w} = \sum_{l=1}^{Nw} \hat{u}_l^w I_l^w T_l(h) \quad (\mathrm{A/m}) \tag{5}$$

where, $\hat{u}_l^w$ is the unit vector of the lth segment along wire antenna, $T_l(h)$ represents a triangular function, and I_l^w is the unknown wire current coefficient of the corresponding segment.

A special attachment mode is introduced wherever wire antenna is connected with the cylinder surface, as shown in Fig. 2, in order to ensure continuity of current flowing from wire antenna to cylinder surface. Then, no discontinuity occurs at any conductive joint part. For a point r in the junction region, the basis function of which is defined as follows

$$\vec{J}^{A}\left(\vec{r}\right) = I^A \begin{cases} \vec{J}_l^a & r \in S_a \\ \vec{J}_d^a & r \in S_d \end{cases} \tag{6}$$

where, $\vec{J}_l^a = \vec{u}_l \frac{T_l^a(h)}{2\pi\, a}$ is the current density on the wire segment nearest the junction region.

$\vec{J}_d^a = -\vec{u}_r \frac{1}{2\pi\, r}\left(\frac{b-r}{b-a}\right)$ is the current density over the cylindrical surface near the junction regions a, and b are the inner and outer radii of the annulus in the junction region, respectively.

Substitute Eq. (3), Eq. (5), and Eq. (6) into Eq. (1). The surface current to each region can be obtained by solving Eq. (1) using Galerkin procedure.

3. IMPEDANCE EXPRESSIONS AND THE EXTRACTING THE SINGULARITY POINT IN THE INTEGRAL

Using Galerkin's method to solve Eq. (1), The general matrix equation can be obtained, with the following form

$$\begin{bmatrix} [Z^{ss}] & [Z^{sw}] & [Z^{sA}] \\ [Z^{ws}] & [Z^{ww}] & [Z^{wA}] \\ [Z^{As}] & [Z^{Aw}] & [Z^{AA}] \end{bmatrix} \cdot \begin{bmatrix} [I^s] \\ [I^w] \\ [I^A] \end{bmatrix} = \begin{bmatrix} [V^s] \\ [V^w] \\ [V^A] \end{bmatrix} \tag{7}$$

In which $[Z^{ss}]$ represents the impedance matrix, which are the familiar impedances defining the EM interactions between various

parts of the revolution body. Similarly, the revolution body-wire, the revolution body-junction, the wire-wire, the wire-junction and junction-junction impedance matrices are denoted by $[Z^{sw}]$, $\left[Z^{sA}\right]$, $[Z^{ww}]$, $\left[Z^{wA}\right]$, and $\left[Z^{AA}\right]$, respectively. $[V^s]$, $[V^w]$, and $\left[V^A\right]$ are the excitation voltage matrix of on the cylinder, the wire, and the junction region, respectively. $[I^s]$, $[I^w]$, and $\left[I^A\right]$ are corresponding surface current to be determined.

The computation of the self impedance matrix and the mutual impedance matrix for the revolution body and wire antenna have been introduced [5–9], the details of this evaluation will not be explained here for brevity. No information on junction region impedance element Z^{AA} is available, here, the impedance of the wire/cylinder surface junction region are carefully treated in a special method.

For the wire/surface junction region self-impedance element Z^{AA}, as shown in Fig. 2, it consists of a small disk basis $\vec{J}_d^a$ on the cylinder surface and a half triangle basis $\vec{J}_l^a$ on the wire. Using Galerkin's method, the self-impedance element at the wire/surface junction region is described as follows

$$\begin{aligned}
Z^{AA} &= \left\langle \vec{W}_l^a, L_a\left(\vec{J}_l^a\right)\right\rangle + \left\langle \vec{W}_d^a, L_a\left(\vec{J}_d^a\right)\right\rangle \\
&\quad + \left\langle \vec{W}_d^a, L_a\left(\vec{J}_l^a\right)\right\rangle + \left\langle \vec{W}_l^a, L_a\left(\vec{J}_d^a\right)\right\rangle \\
&= \frac{jk\eta}{4\pi}\int_0^{h_0} dh' \int_0^{h_0} dh \left\{ T_a\left(h'\right)\cdot T_a\left(h\right)\cdot\left(\vec{u}_a'\cdot\vec{u}_a\right)\right. \\
&\quad \left. -\frac{T_a\left(h'\right)\cdot T_a\left(h\right)}{k^2}\right\}\frac{e^{-jkR}}{R} + \frac{jk\eta}{16\pi^3\left(b-a\right)^2}\int_{-\pi}^{\pi} d\varphi' \int_a^b dr' \int_{-\pi}^{\pi} d\varphi \int_a^b dr \\
&\quad \left\{\left(b-r'\right)\cdot\left(b-r\right)\cdot\left(\vec{u}_r'\cdot\vec{u}_r\right) - \frac{1}{k^2}\right\}\frac{e^{-jkR}}{R} \\
&\quad + \frac{jk\eta}{8\pi^2\left(b-a\right)}\int_0^{h_0} dh \int_a^b dr \int_{-\pi}^{\pi} d\varphi \\
&\quad \left\{T_a\left(h\right)\cdot\left(r-b\right)\cdot\left(\vec{u}_a\cdot\vec{u}_r\right) - \frac{T_a'\left(h\right)}{k^2}\right\}\frac{e^{-jkR}}{R} \\
&\quad + \frac{jk\eta}{8\pi^2\left(b-a\right)}\int_0^{h_0} dh \int_a^b dr \int_{-\pi}^{\pi} d\varphi
\end{aligned}$$

$$\left\{T_a(h)\cdot(r-b)\cdot\left(\vec{u}_a\cdot\vec{u}_r\right)-\frac{T_a'(h)}{k^2}\right\}\frac{e^{-jkR}}{R} \tag{8}$$

3.1. Extracting the Singularity Term in Integral

It can be seen the self-impedance Z^{AA} of the junction region is composed of four terms, the self-impedance between wire antennas, the mutual-impedance between the wire and disk, and the self-impedance between disks. The second term in Eq. (8) is the self-impedance element between disks, which is expressed as Z_{pp}^{AA}. There is a singularity in Z_{pp}^{AA} when $r'\to r$.

$$\begin{aligned} Z_{PP}^{AA} &= \frac{jk\eta}{16\pi^3(b-a)^2}\int_{-\pi}^{\pi}d\varphi'\int_a^b dr'\int_{-\pi}^{\pi}d\varphi\int_a^b dr \\ &\quad\left\{\left(b-r'\right)\cdot(b-r)\cdot\left(\vec{\vec{u}}_r'\cdot\vec{\vec{u}}_r\right)-\frac{1}{k^2}\right\}\frac{e^{-jkR}}{R} \end{aligned} \tag{9}$$

where, $R=\sqrt{r'^2+r^2-2r'r\cos(\varphi-\varphi')}$, $\vec{\vec{u}}_r'\cdot\vec{\vec{u}}_r=\cos(\varphi-\varphi')$.

Let $\begin{cases}\varphi-\varphi'=\alpha\\ \varphi+\varphi'=\beta\end{cases}$, according to the integral domain of Eq. (9), convert the integral domain φ and φ' to α and β, and suppose

$$\begin{aligned} Z\left(r,r'\right) &= \int_{-\pi}^{\pi}d\varphi'\int_{-\pi}^{\pi}d\varphi\left\{\left(b-r'\right)\cdot(b-r)\cdot\cos(\varphi-\varphi')-\frac{1}{k^2}\right\}\frac{e^{-jkR}}{R} \\ &= \frac{1}{2}\int_{\alpha}d\alpha\int_{\beta}d\beta f(\alpha) \\ &= \frac{1}{2}\int_{-2\pi}^{0}f(\alpha)d\alpha\int_{-2\pi-\alpha}^{2\pi+\alpha}d\beta+\frac{1}{2}\int_0^{2\pi}f(\alpha)d\alpha\int_{-2\pi+\alpha}^{2\pi-\alpha}d\beta \\ &= 8\pi\cdot\int_0^{\pi}f(\alpha)d\alpha-2\int_0^{2\pi}f(\alpha)\alpha d\alpha \end{aligned} \tag{10}$$

where

$$f(\alpha)=\left\{\left(b-r'\right)\cdot(b-r)\cdot\cos\alpha-\frac{1}{k^2}\right\}\frac{e^{-jkR}}{R} \tag{11}$$

Suppose $\alpha = 2\pi - \varsigma$, $\cos\alpha = \cos\varsigma$, it can be obtained

$$\int_0^{2\pi} f(\alpha)\alpha d\alpha = \int_0^{2\pi} f(\varsigma)(2\pi - \varsigma)d\varsigma = 2\pi \int_0^{2\pi} f(\varsigma)d\varsigma - \int_0^{2\pi} f(\varsigma)\varsigma d\varsigma \quad (12)$$

So

$$\int_0^{2\pi} f(\alpha)\alpha d\alpha = \pi \int_0^{2\pi} f(\alpha)d\alpha = 2\pi \int_0^{\pi} f(\alpha)d\alpha \quad (13)$$

Substituted Eq. (13) into Eq. (10)

$$Z\left(r, r'\right) = 4\pi \int_0^{\pi} f\left(\alpha\right) d\alpha \quad (14)$$

So the self-impedance term between disks.

$$\begin{aligned} Z_{PP}^{AA} &= \frac{jk\eta}{4\pi(b-a)^2} \int_a^b dr' \int_a^b dr Z\left(r,\, r'\right) \\ &= \frac{jk\eta}{4\pi(b-a)^2} \int_a^b dr' \int_a^b dr \left\{ \left(b - r'\right) \cdot (b - r) \cdot g - \frac{1}{k^2} h \right\} \end{aligned} \quad (15)$$

where

$$g = \frac{1}{\pi} \int_0^{\pi} \frac{e^{-jkR}}{R} \cos\alpha d\alpha \quad (16a)$$

$$h = \frac{1}{\pi} \int_0^{\pi} \frac{e^{-jkR}}{R} d\alpha \quad (16b)$$

using Hanker Function, Eq. (16) can be written as

$$g = \frac{e^{-jkR_0}}{R_0} \left\{ \begin{array}{l} \dfrac{1}{\pi} \displaystyle\int_0^{\pi} \cos\alpha d\alpha + \sum_{m=1}^{\infty} (r' \cdot r)^m \\ \left[\displaystyle\sum_{l=0}^{m} \dfrac{(m+l)!}{m! \cdot l! \cdot (m-l)!} \cdot 2^{-l} (jk)^{m-l} R_0^{-(m+l)} \right] \\ \cdot \displaystyle\int_0^{\pi} \cos^m \alpha \cdot \cos\alpha d\alpha \end{array} \right\} \quad (17a)$$

$$h = \frac{e^{-jkR_0}}{R_0} \left\{ \begin{array}{l} 1 + \sum\limits_{m=1}^{\infty} (r' \cdot r)^m \\ \left[\sum\limits_{l=0}^{m} \frac{(m+l)!}{m! \cdot l! \cdot (m-l)!} \cdot 2^{-l} (jk)^{m-l} R_0^{-(m+l)} \right] \\ \cdot \int_0^{\pi} \cos^m \alpha d\alpha \end{array} \right\} \quad (17b)$$

where, $R_0 = \sqrt{r'^2 + r^2}$ and $(r, r') \in [a, b]$.

So the singularity in integral Eq. (8) can be extracted, and

$$\begin{aligned} Z^{AA} \;=\; & \frac{jk\eta}{4\pi} \int_0^{h_0} dh' \int_0^{h_0} dh \left\{ T_a\left(h'\right) \cdot T_a(h) - \frac{T_a\left(h'\right) \cdot T_a(h)}{k^2} \right\} h \\ & + \frac{jk\eta}{4\pi(b-a)^2} \int_a^b dr' \int_a^b dr \left[\left(b - r'\right) \cdot (b - r) \cdot g - \frac{1}{k^2} \cdot h \right] \\ & + \frac{jk\eta}{2\pi(b-a)} \int_o^{h_0} dh \int_a^b dr \left\{ -\frac{T_a'(h)}{k^2} \right\} h \end{aligned} \quad (18)$$

3.2. Determination the Outer Radius b of the Annulus

The inner radius a of the annulus corresponds to the wire radius, the outer radius b of an annulus is usually chosen to be between 0.1λ to 0.25λ, which has effect on the impedance characteristic, especially on the impedance value of the resonant frequency point. The admittance versus b is calculated in the resonant frequency, as shown in Fig. 3, it can be seen that the admittance converges when the outer radius b is greater than 0.1λ. So we choose $b = 0.107\lambda$ in the paper.

4. VALIDATION OF THE ARITHMETIC

To test the validity of the analysis method above, the impedance characteristic of the wire antenna mounted on a finite solid conducting cylinder is calculated. The dipole which is vertically attached to the surface of the cylinder is shown in Fig. 4(a). The input impedance varying with frequency is shown in Fig. 4(b). It can be seen that the computation result using the developed MOM code is in agreement with the result of the CST commercial software.

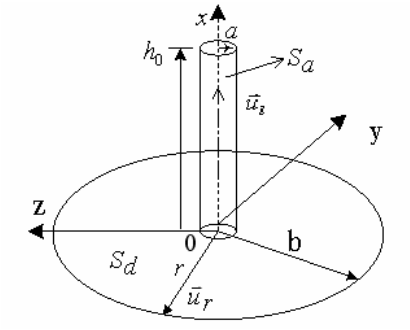

Figure 2. Attachment region at the wire/surface.

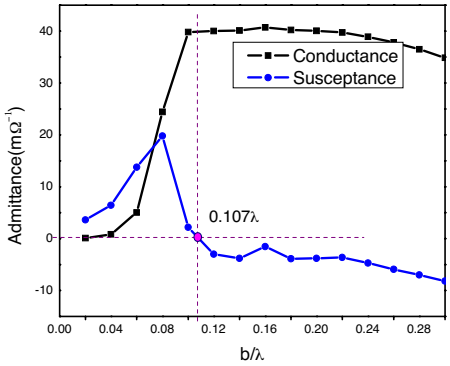

Figure 3. Input admittance of the junction point versus disk radius b.

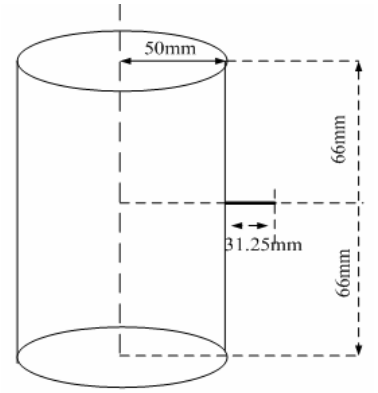

(a)

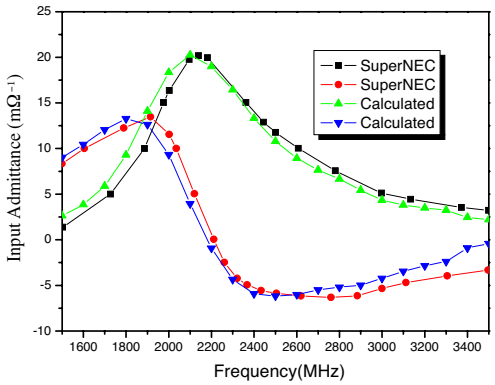

(b)

Figure 4. (a) The dipole vertical the axis of the cylinder. (b) The input admittance vary as the frequency.

In the same way, the impedance and radiation patterns of an L-probe fed patch antenna mounted on a finite solid conducting cylinder are calculated. As shown in Fig. 5(a), when $R_c = 50\,\text{mm}$, $Hc = 132\,\text{mm}$, $L = 44\,\text{mm}$, $W = 44\,\text{mm}$, $s = 14\,\text{mm}$, $s1 = 9.518\,\text{mm}$, $s2 = 20\,\text{mm}$, and the operating frequency is about 2.4 GHz, the impedance characteristic, VSWR and radiation patterns are obtained and as shown in Figs. 5(b)–5(e). The results show pretty good agreement with the results of CST software.

Using the developed MOM code, the patterns of L-probe coupled patch arrays with 8 patch elements is calculated, as shown in Fig. 6(a).

Design parameters of the antenna arrays as following: operating frequency $f = 2.4\,\text{GHz}$, $DR = 100.0\,\text{mm}$, $Hc = 875.0\,\text{mm} = 7\lambda$, $s = 14.0\,\text{mm}$, $s1 = 9.5\,\text{mm}$, $s2 = 20\,\text{mm}$, $Sd = 37.0\,\text{mm}$, patch sizes: $L = 44.0\,\text{mm}$ and $W = 44.0\,\text{mm}$. The results are shown in Fig. 6(b)

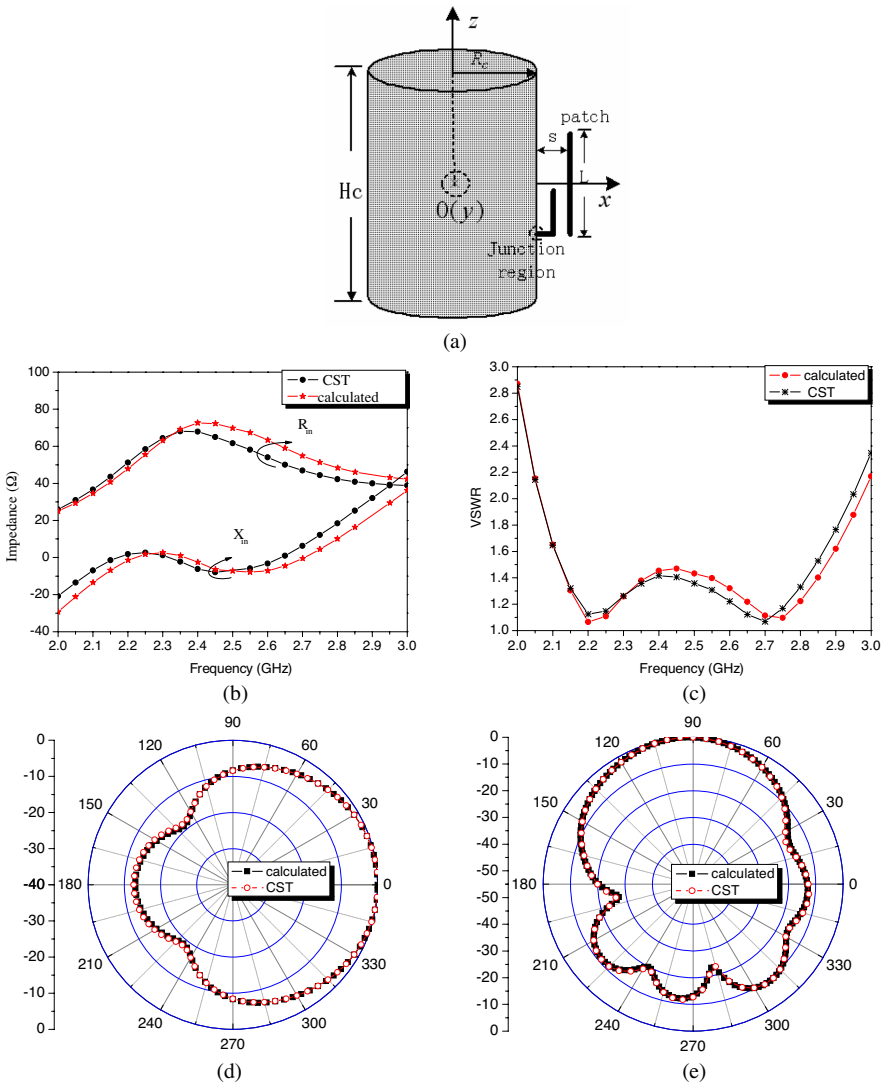

Figure 5. (a) The patch antenna of L-probe feed mounted on metal cylinder. (b) Input impedance versus the frequency. (c) VSWR versus the frequency. (d) The horizontal pattern. (e) The elevation pattern.

and Fig. 6(c), which are in good agreement with the results of the CST software.

Similarly, the radiation patterns of the six elements patch arrays of L-probe feed mounted on cylinder surface are computed. As shown in Fig. 7(a), the six element patch antenna arrays are equally spaced on the cylinder around along circumference, the parameters of the patch and L-probe are as same as in Fig. 6(a), when $R = 86.65\,\text{mm}$, $H = 132\,\text{mm}$, $Sp = 62.5\,\text{mm}$, and the operating frequency is also about 2.4 GHz. The radiation patterns are calculated and showed in Fig. 7(b) and Fig. 7(c). The results are also in pretty good agreement with the results of CST software.

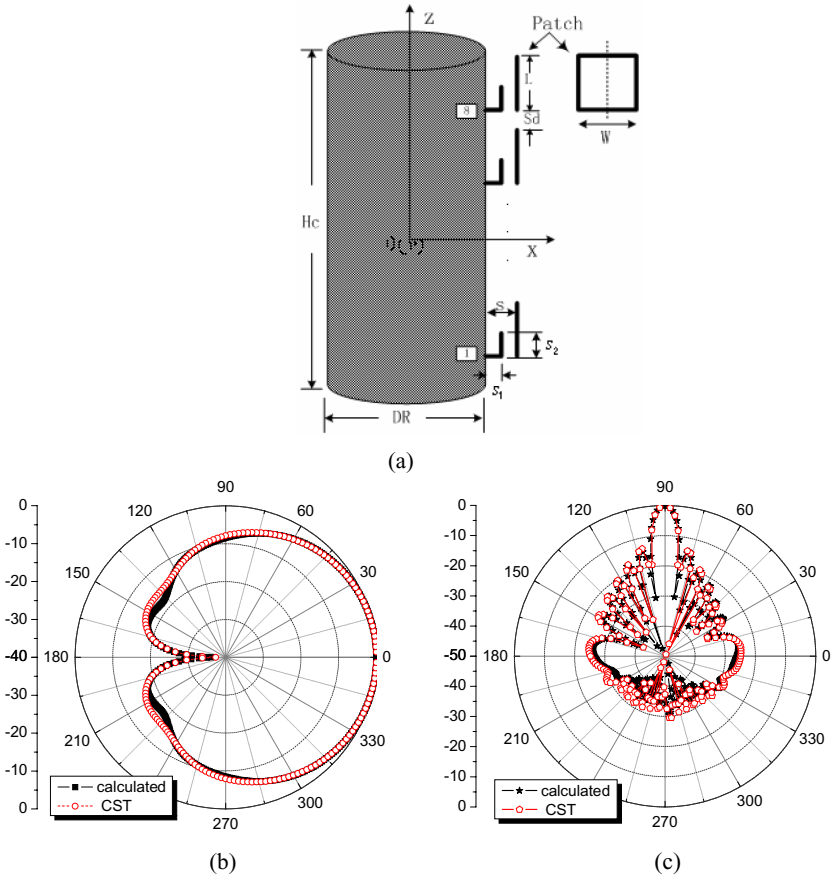

Figure 6. (a) Geometry of the eight-element patch antenna array mounted on a cylinder. (b) The horizontal pattern. (c) The elevation pattern.

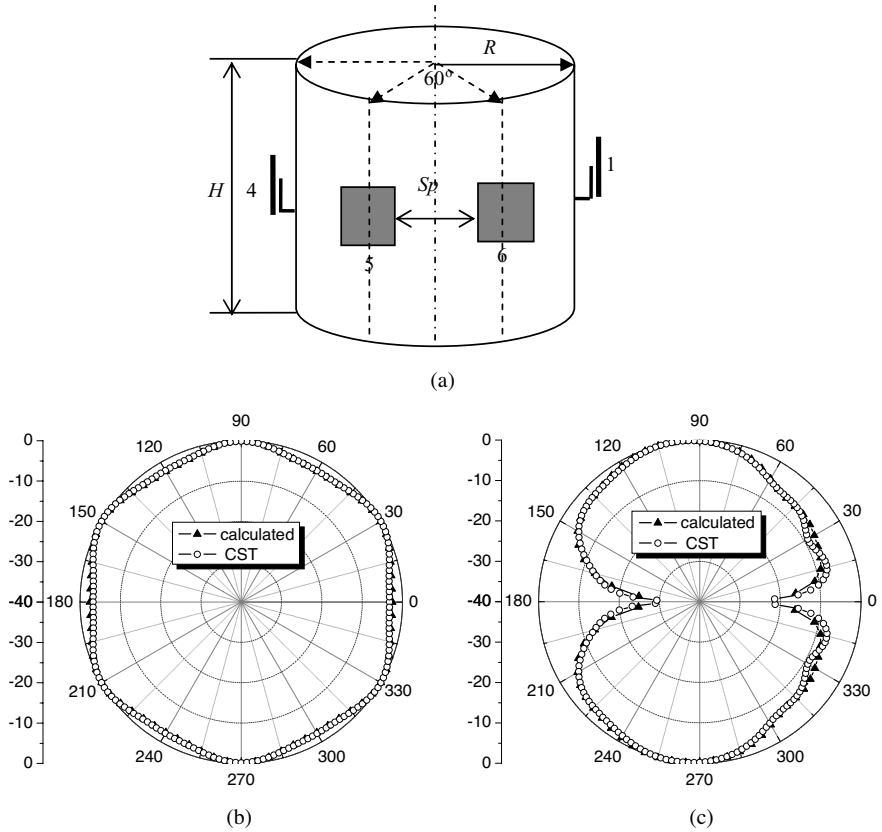

Figure 7. (a) The six elements patch antenna arrays of the L-probe feed with body of cylinder. (b) The horizontal pattern. (c) The elevation pattern.

5. CONCLUSION

In the paper, taking wire antenna problem with body of revolution as an example, the exact analysis model and computation method using MOM in conjunction with the electric field integral equation is proposed. The basis function is set up in terms of the geometry characteristic of revolution body, in order to reduce the element number of the impedance matrix and speed up the impedance matrix computation. The special basis function is introduced at junction region between the metal wire and the cylindrical surface, so as to ensure the continuity of current density. The integral transform is introduced and the computation formula of the self-impedance element

at the junction region between the metal wire and the cylinder surface is carefully derived to extract the singularity and a relatively accurate solution is obtained. The examples above show that the method in this paper is accurate and efficient. The analytical technique developed in this paper can be used to study electromagnetic radiation and scatter problems of wire antenna and array attached to bodies of revolution.

ACKNOWLEDGMENT

The work described in this paper was fully supported by National Natural Science Foundation of China (Program No. 60671001).

REFERENCES

1. Cao, X., P. Li, K. M. Luk, and C. Liang, "Efficient analysis of L-probe coupled patch antenna arrays mounted on a finite conducting cylinder," *Microwave and Optical Technology Letters*, Vol. 41, No. 5, 403–407, 2004.
2. Cao, X., J. Qin, K. M. Luk, and C. Liang, "The efficient analysis model of antenna with bodies of revolution," *Microwave & Millimetre-wave Symposium of China (2005CNMWS)*, 420–424, 2005.
3. Harrington, R. F., *Field Computation by Moment Methods*, New York, Macmillan.
4. Mautz, J. R. and R. F. Harrington, "Radiation and scattering from bodies of revolution," *Appl. Sci. Res.*, Vol. 20, 405–435, 1969.
5. Andreasen, M. G., "Scattering from bodies of revolution," *IEEE Trans. Antennas Propagat.*, Vol. 13, 303–310, 1965.
6. Medgyesi-Mtschang, L. N. and J. H. Mullen, "Radiation and scattering from asymmetrically excited bodies of revolution," *IEEE Trans. Antennas Propagat.*, Vol. 24, No. 1, 90–93, 1976.
7. Gedney, S. D. and R. Mittra, "The use of the FFT for the efficient solution of the problem of electromagnetic scattering by a body of revolution," *IEEE Trans. Antennas Propagat.*, Vol. 38, No. 3, 313–321, March 1990.
8. Raquel, P. L. and F. C. Manuel, "Input impedance of wire antennas attached on-axis to conducting bodies of revolution," *IEEE Trans. Antennas Propagat.*, Vol. 36, No. 9, 1236–1243, 1988.
9. Jung, H. and C. Seo, "Characteristics of circular polarization of ellipitical microstrip antenna with full-wave analysis considering

the attachment mode," *Microwave and Optical Technology Letters*, Vol. 22, No. 2, 111–114, 1999.

10. Tarricone, L., M. Mongiardo, and F. Cervelli, "A quasi-one-dimensional integration technique for the analysis of planar microstrip circuits via MPIE/MOM," *IEEE Trans. Microwave Theory Tech.*, Vol. 9, No. 3, 517–522, 2001.